

Interactions between Dead-Beat Controlled High-Quality Rectifiers and Input Filters

P. Mattavelli

S. Buso

University of Padova
Department of Electrical Engineering
Via Gradenigo 6/A - 35131 Padova - ITALY
E-Mail: pmatta@tania.dei.unipd.it

University of Padova
Department of Electronics and Informatics
Via Gradenigo 6/A - 35131 Padova - ITALY
E-Mail: simone@tania.dei.unipd.it

Abstract - The paper analyses the stability limitations of the digital dead-beat current control applied to voltage-fed three-phase converters used as PWM rectifiers. In particular, attention is focused on the interactions between the rectifier and the input filters, which are commonly employed to eliminate the high frequency harmonic content from the line currents. The effects of the inherent model mismatch represented by the input filters, which are not normally included in the conventional dead-beat algorithm, are analysed by developing a detailed stability analysis, based on a discrete-time state space model of the controlled system. The proposed analysis allows to predict the occurrence of unstable conditions and to identify some control refinements improving the system's robustness. The results of the theoretical analysis and the validity of the proposed modifications to the control strategy are finally verified by simulations.

Keywords: converter control, switched mode power supplies, three phase systems

1. INTRODUCTION

The use of fully digital control techniques for PWM converters is, more and more often, the preferred design choice thanks, on the one hand, to the well known advantages of the digital controls in terms of flexibility, insensitivity to ageing effects and/or thermal drifts, ease of implementation and upgrade, and, on the other hand, to the availability of powerful, low-cost microcontrollers (μ C's) and digital signal processors (DSP's). This paper focuses on the stability limits of the dead-beat current control technique [1]-[3], since this is a widely applied digital current control technique for power converter applications, such as PWM rectifiers.

In particular, the paper analyses the interactions between a dead beat controlled PWM rectifier and the input passive filters which are normally adopted to reduce the high frequency harmonic content of the current injected on the utility grid. The dynamics of these filters are not normally taken into account in the conventional dead-beat current control algorithm, which is directly derived from drive applications. This causes an

inherent mismatch between the internal representation of the load applied to the rectifier and the actual one. While the dead-beat control's algorithm is capable of providing a satisfactory dynamic performance when the converter's ac impedances are exactly identified, in case of a not correct identification, stability problems may arise [2]. More specifically, the presence of model mismatches or, in case of a correctly identified model's structure, of parameter uncertainties and/or variations can cause stability problems to the current control loop, especially when a line voltage estimation strategy is adopted, as reported in [2]. This paper extends the analysis of the problem, as presented in [5]-[6], deriving a generalized discrete-time state-space representation of the controlled converter and its load, which includes also the input filters. The analysis procedure reveals the stability margins of the algorithm considering its typical implementation, which employs a conventional line voltage estimation technique, and gives the possibility of predicting the occurrence of oscillations in the current loop by mapping the closed loop plant's eigenvalues. Besides, a modification to the control algorithm is proposed, which is shown to increase the

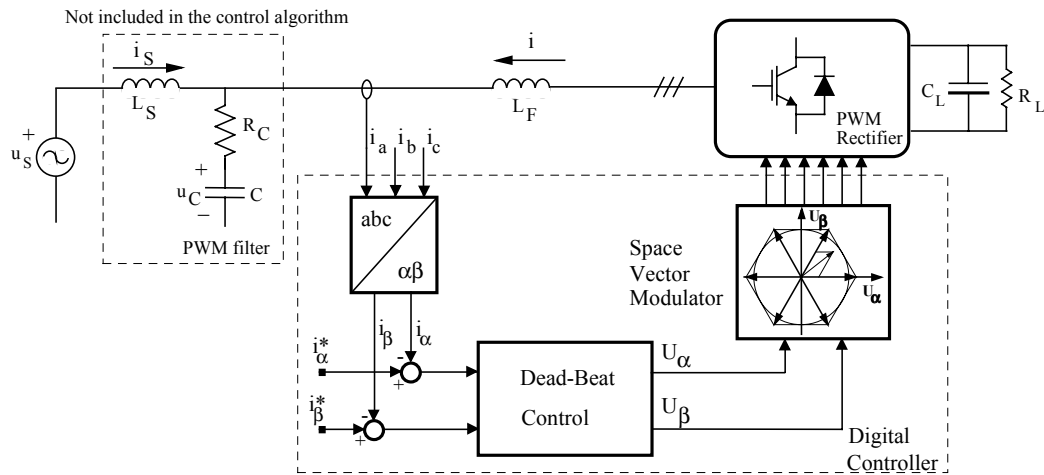


Fig. 1 - Simplified representation of a PWM rectifier using a digital dead-beat current regulator.

control's robustness. All the theoretical forecasts are verified by means of simulations.

2. BASIC SCHEME OF THE SYSTEM

The basic scheme of a PWM rectifier, which is the application discussed in this paper, is shown in Fig. 1. As can be seen, for the sake of simplicity, the power converter feeds a generic resistive load R_L on the DC side. The passive components L_S , C are required to filter the current high frequency harmonic components which are due to the modulation process and must be suitably damped to avoid undesired resonant oscillations of the line current i_s . Resistor R_C , also shown in Fig. 1, indicates one of the possible configurations to smooth the resonance of the input filter. Actually, it may be substituted by an active damping obtained by a proper control of the PWM converter [8], if the oscillation frequency falls within the current control bandwidth. Finally, it may be worth noting that in L_S also the line impedance is included. As a matter of fact, depending on the particular application requirements, a series filter inductance may not be necessary and inductance L_S of Fig. 1 represents the line impedance only; this is, indeed, the case assumed in the analysis discussed in 3.3.

It is assumed that the control of the PWM converter's current is performed by means of the dead-beat control technique [1]-[7]. As it is well known, in a dead-beat controller the control algorithm calculates the voltage to be generated by the power converter so as to make the phase current reach its reference by the end of the following modulation period. The necessary

calculations are typically performed in the α , β frame, and the space vector modulation (SVM) strategy, which very well suits the digital implementation, is adopted for the switching converter. An important advantage of the dead-beat technique is that it does not require the line voltage measurement in order to generate the current reference. The dead-beat control's algorithm, in fact, allows an estimation of the line voltage instantaneous value, based on the data measured in the previous modulation periods, which can therefore be used also for the current reference generation. On the other hand, the inherent delay due to the calculation time is indeed a serious drawback of this control technique, which implies an unavoidable tracking error between the current reference and the actual generated current. In the more recent versions [2] of the dead-beat controller, the delay is reduced by sampling the control variables and executing the control routines twice in a modulation period. The turn-on and turn-off times of the power converter switches are independently decided in two successive control intervals. As a consequence, the aforementioned delay in the current reference tracking can be reduced to a single modulation period. In the following analysis, a basic implementation of the dead-beat algorithm is considered, this being the more commonly used. The same approach may, of course, be applied also to the double sampled version of the algorithm by simply modifying the sampling period and the discretized equations accordingly.

3. STABILITY ANALYSIS

Dead-beat control of three-phase inverters has been widely investigated by many researchers in recent years [1]-[5], especially for drive applications. The application of the same control technique to active filters or PWM rectifiers is almost straightforward; however, as stated before, the effect of the input filters must be carefully considered. These filters, in fact, are not normally accounted for in the control algorithm, which refers to an "ideal" load model, where only inverter inductances L_F are taken into account, as indicated by the dashed box in Fig. 1. This is what can be called a *model mismatch*. The direct approach to solve this problem, that is to augment the internal load model so as to include the input filter dynamics, is not practically adopted for different reasons: the basic ones are the dependence of the dynamics on the line impedance, which is normally unknown, and the complexity of the resulting control algorithm, which is generally unacceptable.

Even if the model mismatch is avoided, because the structure of the load seen by the rectifier is correctly identified, problems may arise when there is a *parameter mismatch*, in particular between the modeled inverter inductance and the actual one [2].

Moreover, in active filters and high-quality rectifiers the *line current reference generation* is related to the line voltage, introducing an additional action which may affect the system's stability. All of these points are hereafter analyzed separately, beginning from the parameter mismatch case.

3.1. Analysis of parameter mismatches [6]

We first consider the case in which the presence of the line impedance and of the input filter are neglected. Stability analysis is performed using the discrete-time state space equations of the remaining first order system, given by the actual converter inductances L_F . Note the three-phase system is assumed to be balanced and symmetrical. As a consequence, the discrete time system equations, developed in the α , β fixed reference frame, have the following expression:

$$i(k+1) = \frac{T_{sw}}{L_F} [u_{av}(k) - u_s(k)] + i(k), \quad (1)$$

where $i(k)$ is the inverter current, $u_{av}(k)$ the average phase voltage generated by the rectifier, and $u_s(k)$ the supply voltage, all of them evaluated at the sampling instant kT_{sw} .

The control algorithm, which ensures a dead-beat response for the first order system based on the modeled inductance L_m is given by [1]-[6]:

$$u_{av}(k+1) = \frac{L_m}{T_{sw}} [i_{ref}(k) - i(k)] + 2u_s(k) - u_{av}(k), \quad (2)$$

where the line voltage u_s is either measured or estimated. The line voltage estimation can be obtained using the algorithm:

$$e_s(k-1) = u_{av}(k-1) + \frac{L_m}{T_{sw}} [i(k-1) - i(k)] \quad (3)$$

and then substituting in (2) $u_s(k)$ with $e_s(k-1)$ [1]-[5].

The stability analysis of the closed loop system can be performed by applying the Z-transform to (1), (2) and possibly (3), by deriving the characteristic polynomial of the closed loop system, and by mapping the closed loop poles. If the magnitude of the closed loop poles is equal or greater than one, the resulting system is, of course, unstable.

Following this procedure, it can be found that, if the line voltage is measured, the poles of the closed loop system given by (1) and (2) are:

$$p_{1,2} = \pm \sqrt{\Delta L\%}, \quad (4)$$

where $\Delta L\% = 1 - L_m/L_F$ is the relative error between the actual and the modeled inductance. Eq. (4) shows that the system's stability is ensured up to 100% error in the modeled inductor L_m , revealing a considerable robustness to parameter mismatches for this condition. It is worth noting that only positive values of $\Delta L\%$ will be presented throughout the analysis, since this reveals that negative values always imply a somewhat higher stability margin. Therefore, positive errors (implying an underestimation of L_F) have been considered as the worst case.

Instead, if the line voltage is estimated using (3), it turns out that the characteristic polynomial of the closed loop system, determined by (1), (2) and (3), is

$$\lambda(z) = z^3 - 3\Delta L\% z + 2\Delta L\%. \quad (5)$$

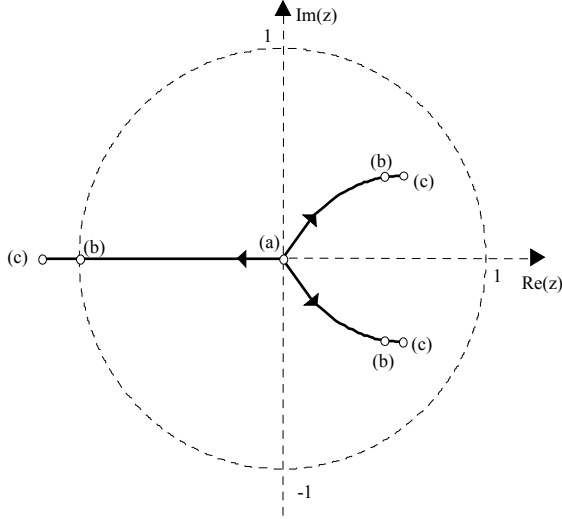


Fig. 2 - Real and imaginary components of the closed loop poles for different values of $\Delta L_{\%}$ parameter: (a) $\Delta L_{\%} = 0\%$, (b) $\Delta L_{\%} = 20\%$, (c) $\Delta L_{\%} = 30\%$.

The closed loop poles, obtained solving $\lambda(z)=0$ and reported in Fig. 2, show that only a 20% error is allowed before system instability occurs. It is worth noting that this result is independent of the switching frequency since (5) is only function of the relative error $\Delta L_{\%}$. Moreover, it is interesting to note that the unstable pole is at half of the switching frequency since it lies on the real axis of Fig. 2.

3.2. Analysis with model mismatch

Let us now consider the state space equations of the complete system of Fig. 1. The continuous time system equations, again developed in the α , β fixed reference frame, assuming a three-phase balanced and symmetrical system, have the following expressions:

$$\frac{d\bar{x}}{dt} = A \cdot \bar{x} + \begin{bmatrix} \frac{1}{L_F} \\ 0 \\ 0 \end{bmatrix} \cdot u_{av} + \begin{bmatrix} 0 \\ \frac{1}{L_S} \\ 0 \end{bmatrix} \cdot u_s \quad (6)$$

$$\bar{x} = \begin{bmatrix} i \\ i_s \\ u_c \end{bmatrix}, \quad A = \begin{bmatrix} -\frac{R_c}{L_F} & -\frac{R_c}{L_F} & -\frac{1}{L_F} \\ \frac{R_c}{L_S} & -\frac{R_c}{L_S} & \frac{1}{L_S} \\ \frac{1}{C} & \frac{1}{C} & 0 \end{bmatrix}$$

where $i_s(t)$ is the line current, $u_c(t)$ the voltage on the switching frequency filter, and $u_s(t)$ the internal supply voltage, while R_c is the damping resistor. Discrete time system equations are

obtained by using a zero-order-hold sampling (at instant kT_{sw}) of the continuous time system (6). Indeed, the use of the average phase voltage $u_{av}(t)$, instead of the actual one, is an approximation which is negligible only if we assume that the natural frequencies of system (6) are much lower than the sampling frequency.

Assuming that the control algorithm is not changed, despite the presence of the input filter, (2) and (3) are still valid. Stability analysis of the closed loop system can be performed, as in the previous case, by applying the Z-transform to (6), (2) and possibly (3), by deriving the characteristic polynomial of the closed loop system, and by mapping the closed loop poles. If the input filter voltage is measured, the poles of the closed loop system given by (6) and (2) are shown in Fig. 3, which has been obtained using the following parameters: $L_F = 0.043$ pu, $L_S = 0.02$ pu, C ranging from 0.005 pu to 0.5 pu, $R_C = 0$, $T_{sw} = 100 \mu s$, (we assume hereafter that the base quantities are: nominal power $P_b = 10$ kVA, phase-to-phase voltage $V_b = 380$ V_{RMS}, base frequency $f_b = 50$ Hz). It is interesting to note that increasing filter capacitor C , system poles move close to the ideal condition where two poles are in the origin (eq. (4)) and two poles represent the dynamics of the uncontrolled input filter. Instead, decreasing the value of filter capacitor C , two poles shift toward the unity circle and the system can even become unstable.

If the line voltage is estimated using (3), the

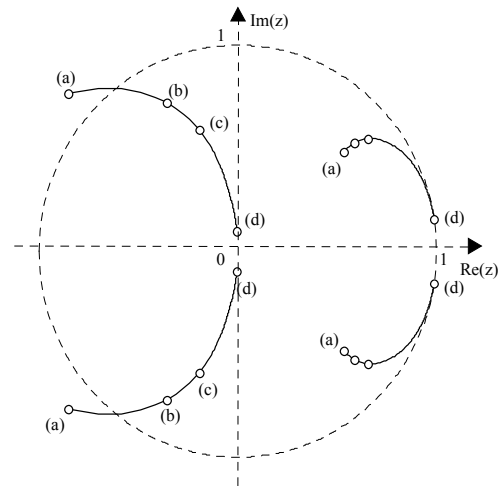


Fig. 3 - Real and imaginary components of the closed loop poles for different values of capacitor C : (a) $C = 0.005$ pu, (b) $C = 0.01$ pu, (c) $C = 0.015$ pu, (d) $C = 0.5$ pu.

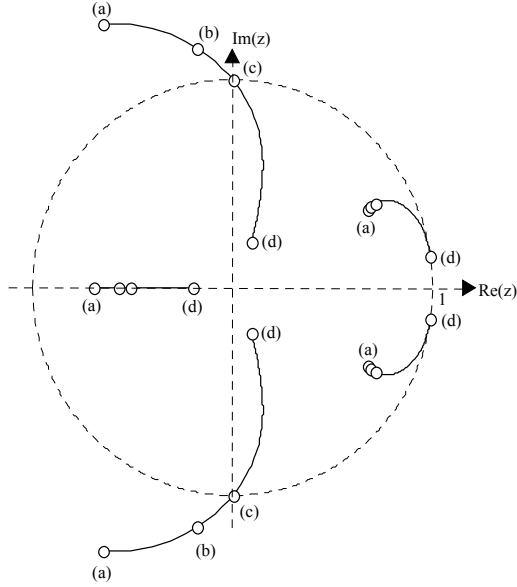


Fig. 4 - Real and imaginary components of the closed loop poles for different values of capacitor C : (a) $C = 0.005$ pu, (b) $C = 0.01$ pu, (c) $C = 0.015$ pu, (d) $C = 0.5$ pu.

poles of the closed loop system given by (6) and (2) are shown by the map of Fig. 4, which is obtained using the same parameters of the previous one. Note that we have an additional pole on the real axis, associated with the estimation algorithm (3) and that the unstable condition can be reached even for capacitor values smaller than 0.015 pu.

We note that capacitor values, which may give unstable operation, are slightly smaller than the typical filters used in these applications. As a consequence, dead-beat current controlled inverters may require only a small oversizing of the filter capacitor to achieve satisfactory dynamic responses.

3.3. Generation of the current reference

A significant change in the system behaviour is obtained when the rectifier current reference $i_{\text{ref}}(k)$ is a function of the line voltage estimation $e_s(k-1)$:

$$i_{\text{ref}}(k) = -G_{\text{eq}} e_s(k-1). \quad (7)$$

Indeed, this provision, which avoids the use of the line voltage sensors, is peculiar of active filters and high-quality rectifiers, where the line current reference is related to the line voltage, and is not encountered in drive applications.

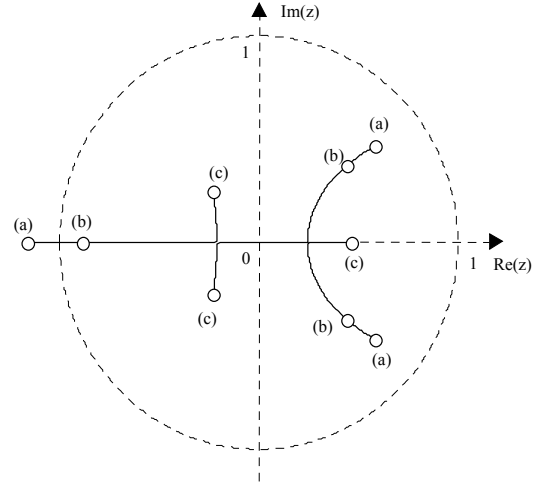


Fig. 5 - Real and imaginary components of the closed loop poles for different values of the equivalent conductance G_{eq} : (a) $G_{\text{eq}} = -1$ pu, (b) $G_{\text{eq}} = 0$, (c) $G_{\text{eq}} = 1$ pu.

Even if we neglect the presence of the input filter dynamics, (7) may strongly affect system's stability in the presence of parameter uncertainties [6]. We recall [6] that critical conditions are encountered when G_{eq} is negative, i.e. for those applications in which the power converters are injecting active power into the line, where the maximum allowed error $\Delta L\%$ is drastically reduced. As an example, Fig. 5 shows the closed loop poles obtained using $\Delta L\% = 0.15\%$ and varying the equivalent conductance G_{eq} from -1 pu to 1 pu. It is worth noting that one pole moves toward the unity circle when G_{eq} becomes negative and, again, the unstable mode due to the parameter uncertainties is at half of the switching frequency.

A different type of instability may arise when the dynamics of the input filters are included and when the PWM rectifier current reference $i_{\text{ref}}(k)$ is determined through (7). In fact, even neglecting parameter mismatch, we have seen that, using (7) into (2) and applying the Z-transform to (2), (3), and the sampled version of (6), the closed loop poles may have magnitude greater than one for negative values of G_{eq} and these unstable modes, if present, oscillate at frequencies close to the input filter oscillation frequency given by C and L_S . As an example, Fig. 6 shows the closed loop poles' map obtained using $L_F = 0.043$ pu, $L_S = 0.04$ pu, $C = 0.1$ pu ($R_C = 0.19$ pu), $\Delta L\% = 0$ and varying the equivalent conductance G_{eq} from -1 pu to 1 pu. As G_{eq} becomes negative, the poles associated

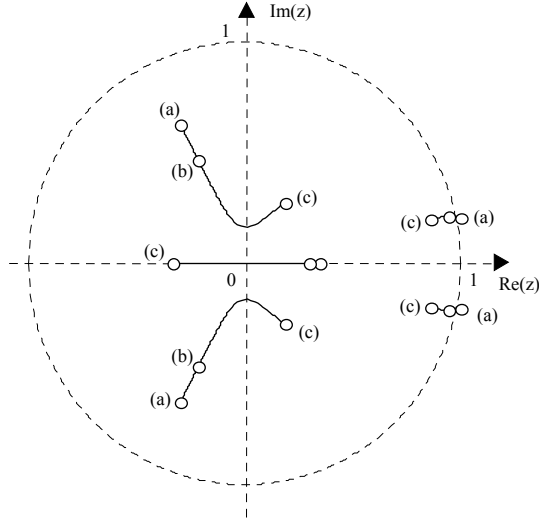


Fig. 6 - Real and imaginary components of the closed loop poles for variation of equivalent conductance G_{eq} : (a) $G_{eq} = -1$ pu, (b) $G_{eq} = 0$, (c) $G_{eq} = 1$ pu.

with the input filter dynamics move toward the unity circle, crossing it for $G_{eq} = -0.45$ pu.

Indeed, this second type of instability can be explained with a simplified reasoning, highlighting a potential problem which is general for any current controlled PWM rectifier working in the regenerative mode. The system can be schematically represented as in Fig. 7, where a current generator is used to represent the current controlled rectifier. The generator current is supposed to be given by (8), where the current reference given by (7) is multiplied by the closed loop transfer function of the current controller, which can be roughly approximated by a low pass filter with a suitably placed single pole. This should simply represent the dead-beat control delay in the current reference tracking. Note that it is assumed to have a measurement of the output voltage u_{CT} ; therefore no estimation algorithm is taken into account.

$$i(s) = -G_{eq} \cdot u_{CT}(s) \cdot \text{Reg}_I(s) \quad (8)$$

Referring to Fig. 7, it is easy to determine the open loop gain of the system $GH(s)$, which is given by (9). The root locus plot for (9), which is shown in Fig. 8, reveals that, as already anticipated by the general analysis, instabilities in the system may arise as the value of G_{eq} goes negative and lower than a minimum value, which can be found to be around -0.5. This is in good agreement with the critical value $G_{eq} = -0.45$, which was previously determined.

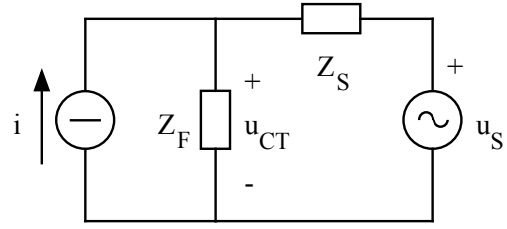


Fig. 7 - Equivalent scheme of the rectifier.

$$GH(s) = G_{eq} \cdot \frac{Z_S(s) \cdot Z_F(s)}{Z_S(s) + Z_F(s)} \cdot \text{Reg}_I(s) \quad (9)$$

It is worth noting that this kind of instability does not depend on the particular implementation of the current controller, but is inherent in the regenerative operation of the converter when a capacitive filter is located at the output, as it is usual. Therefore, the outer control loop, which produces the current reference, has to be corrected to improve the stability in this particular condition. A simple way to implement such a correction is discussed in the following section.

4. ROBUSTNESS IMPROVEMENT

First we want to address the problem of the low frequency instability arising in the system because of the interaction between the current controlled rectifier and the input capacitive filter, which, as it has just been demonstrated in section 3.3, is particularly critical in the regenerative mode of operation. This interaction is made possible by the current reference generation strategy, which uses the measured or estimated line voltage to build the current reference. The direct coupling between the current reference and the line voltage allows the possible instabilities

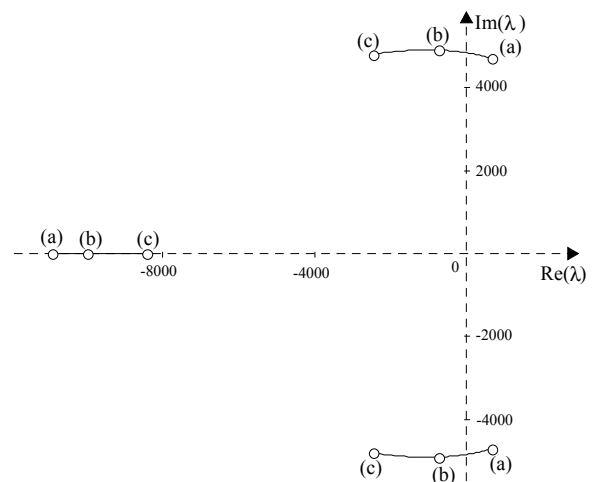


Fig. 8 - Root locus: (a) $G_{eq} = -1$ pu, (b) $G_{eq} = 0$, (c) $G_{eq} = 1$ pu.

to propagate through the system. A possible solution is based on the fact that these instabilities occur at the resonance frequency of the input capacitive filter and the inductive line impedance, which is normally much higher than the supply frequency. It is therefore possible to eliminate the coupling between the line voltage and the current reference generator using a filter on the estimated (or measured) voltage $e_s(k)$ (or $u_s(k)$), which selectively returns to the current reference generator only the fundamental frequency component of the line voltage. The block diagram corresponding to the proposed control implementation is shown in Fig. 9a, in the case of line voltage estimation.

Since the line voltage $u_s(t)$ can be considered almost sinusoidal at a fixed frequency, a proper choice for the selective filter is a digital band-pass filter centered at the supply frequency

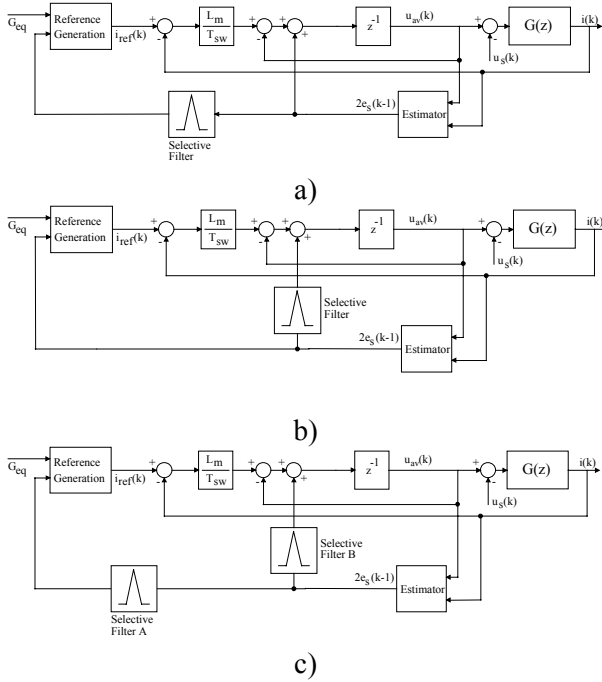


Fig. 9 - Control system modifications:

- selective filter inserted between estimation of the line voltage and current reference generation. $G(z)$ is the discrete time transfer function of the rectifier load.
- selective filter inserted between estimation of the line voltage and current control.
- selective filters inserted between the line voltage estimation algorithm and both the current reference generation and the current control algorithms.

whose expression is given by (10), where: $\lambda \Leftarrow 2\pi f_b T_s$, $f_b = 50\text{Hz}$ (filter frequency equal to the line frequency), $T_s = 100\mu\text{s}$ (sampling period), and m is the filter resonant poles' magnitude.

$$W(z^{-1}) = \frac{2 \cos \lambda (1 - m) z^{-1} + (m^2 - 1) z^{-2}}{1 - 2m \cos \lambda z^{-1} + m^2 z^{-2}} \quad (10)$$

Secondly, we consider the problem of the high frequency instability, arising in the case of a parameter mismatch, as discussed in section 3.1. Basically the same idea adopted for the previous case can here be applied. Again, the origin of the instability is the interaction between the estimation algorithm (3) and the current control algorithm (2). These algorithms can be decoupled from each other by using a suitably designed selective filter, as shown in Fig. 9b. In this case the instability frequency is the half of the switching frequency; therefore, a low pass filter capable of eliminating this high frequency content from the estimated voltage while maintaining the low frequency part of the signal, would, in principle, be a good choice. Nevertheless a band-pass filter centered on the line frequency can do the same job, while minimizing the phase-shift at the supply frequency. This filter does not need to be very selective, which can be an advantage in the case of sudden variation of the input voltage (e.g. voltage sags). A very selective filter, having a

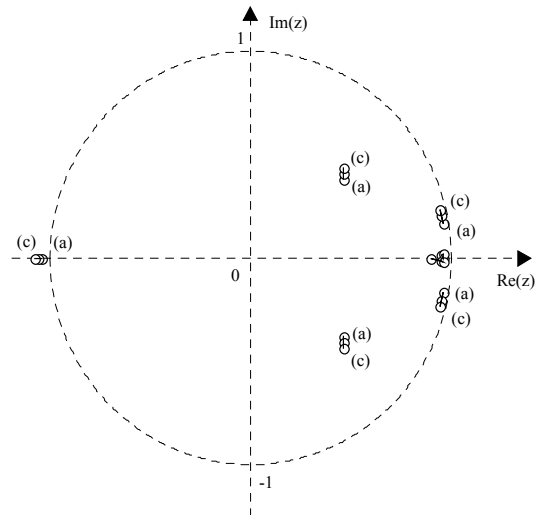


Fig. 10 - Real and imaginary components of the closed loop poles with $\Delta L_{\%} = 25\%$ and different values of equivalent conductance G_{eq} : (a) $G_{eq} = -1$ pu, (b) $G_{eq} = 0$, (c) $G_{eq} = 1$ pu.

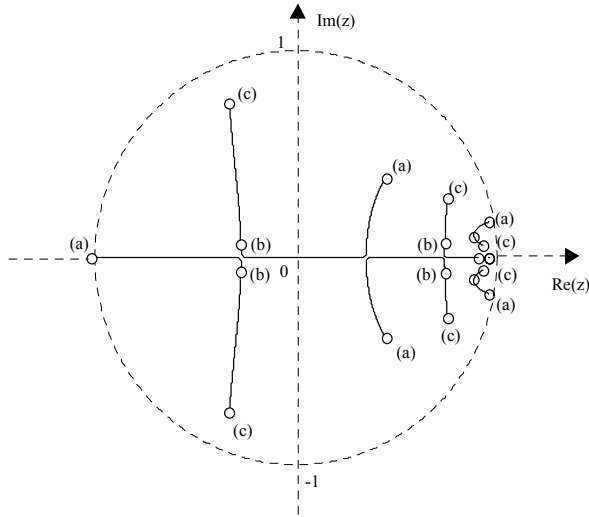


Fig. 11 - Real and imaginary components of the closed loop poles with $\Delta L_o=25\%$ and different values of equivalent conductance G_{eq} : (a) $G_{eq} = -1$ pu, (b) $G_{eq} = 0$, (c) $G_{eq} = 1$ pu.

long settling time, could indeed worsen the current loop dynamic speed of response to input voltage variations; a less selective one, instead, can achieve the needed decoupling while giving a faster response.

We finally consider the case in which both the decoupling actions have to be implemented, because regenerative mode of operation and parameter mismatches are expected in the particular application. It is of course possible to insert both the selective filters in the control system, as shown in Fig. 9c, but another possibility must be considered. A single filter inserted at the output of the estimation algorithm can indeed perform both tasks, but it is necessary to accept a certain degradation of the current loop performance due to the selectivity required to decouple the current reference generation from the estimation algorithm.

The effects of these modifications can be appreciated by evaluating the map of the system's poles in the three cases. The solution of Fig. 9a) determines the map depicted in Fig. 10. As can be seen, the position of the poles due to the input filter is almost unchanged varying the G_{eq} value. Nothing happens to the poles due to the parameter mismatch that are almost unchanged too. Therefore, if a significant mismatch can be expected (higher than 20%), this solution is not capable of guaranteeing the

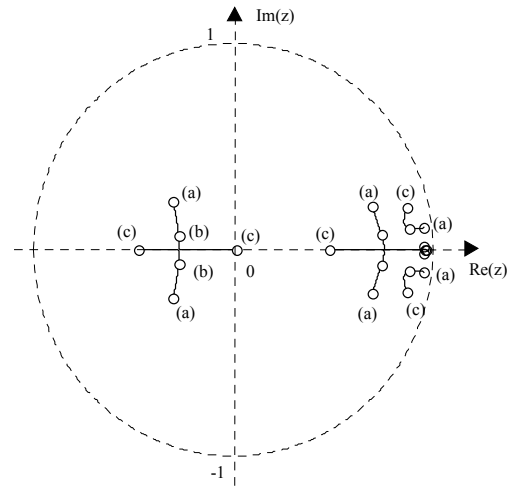


Fig. 12 Real and imaginary components of the closed loop poles with $\Delta L_o=25\%$ and different values of equivalent conductance G_{eq} : (a) $G_{eq} = -1$ pu, (b) $G_{eq} = 0$, (c) $G_{eq} = 1$ pu.

stability of the system. As shown in the figure, which refers to a 25% mismatch, the system is unstable. Nevertheless, if the filter inductance is correctly estimated and therefore the poles associated to the mismatch stay within the unity circle, this provision surely solves the problem in the regenerative mode of operation.

The solution of Fig. 9b, determines the pole map shown in Fig. 11. As can be seen, the poles' positions are not fixed and still an instability problem can be expected. This is due to the interaction which is still present between the estimation and the current control algorithms which propagates through the current reference generation. Therefore, this solution is not a practically viable one.

The solution of Fig. 9c determines the pole map of Fig. 12, where, the poles' positions appear to be almost insensitive of the parameter mismatch and G_{eq} variations. Therefore this is the solution which can be practically considered the most effective. The only drawbacks are the necessity to use two different filters or, if only one at the output of the estimation algorithm is implemented, the necessity to degrade the current loop performance in the presence of voltage fluctuations.

5. SIMULATION RESULTS

The system of Fig. 1 has been simulated in order to verify the results of the described mathematical analysis and the effectiveness of

the suggested modifications. The system's parameters are: $L_F = 2 \text{ mH}$, $C = 15 \text{ } \mu\text{F}$, $R_C = 4 \text{ } \Omega$, $L_S = 1 \text{ mH}$, the phase-to-phase voltage is $380 \text{ V}_{\text{RMS}}$, the nominal power of the load is 10 kW and the switching frequency is 20 kHz .

Fig. 13 reports an example of instability which occurs due to the oscillation between the PWM filter and the line impedance generated by (7) using the conventional estimation technique and neglecting the parameter mismatch (i.e. $\Delta L_{\%} = 0$). Note that the unstable conditions take place when the rectifier is working in regenerative mode, as predicted by our analysis. We also verified that, if the filter voltage is measured instead of being estimated, the unstable condition is still present and the results of Fig. 13 do not change significantly. Moreover, we have also verified that, when parameter errors are taken into account (i.e. $\Delta L_{\%} \neq 0$), even worse stability problems can be encountered. Fig. 14, instead, shows the main rectifier waveforms in the same operating condition of Fig. 13, but using a pass band filter (with $m = 0.9$) for the generation of the current reference. With the adopted provision, the system becomes stable and the dynamic response well damped even in regenerative operating mode.

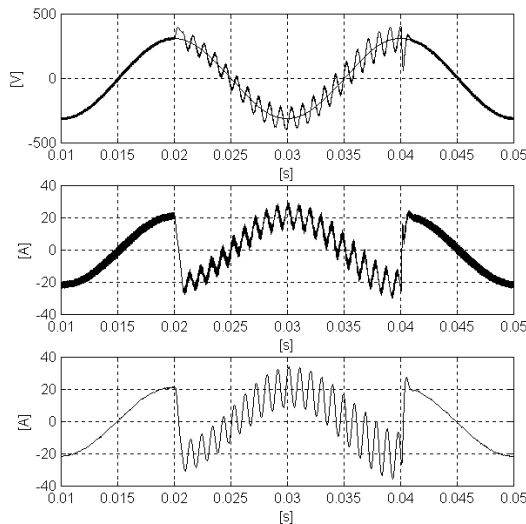


Fig. 13 - PWM rectifier behaviour with the conventional estimation technique and using (7) and $\Delta L_{\%} = 0$. Upper trace: line voltage (u_S) and filter voltage (u_C). Middle trace: converter output current ($-i_F$). Lower trace: line current (i_S).

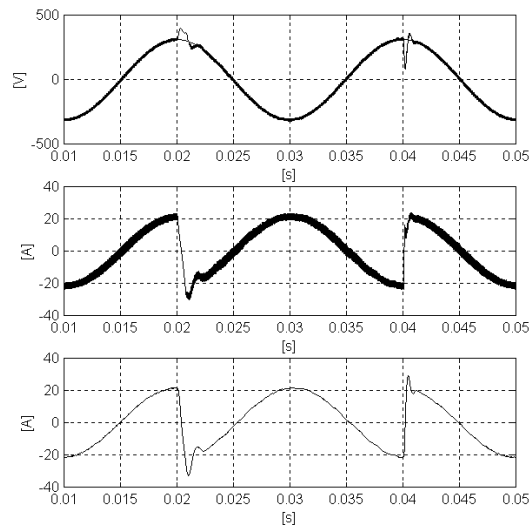


Fig. 14 PWM rectifier behaviour using the proposed solution and $\Delta L_{\%} = 0$. Upper trace: line voltage u_S and filter voltage (u_C). Middle trace: converter output current ($-i_F$). Lower trace: line current (i_S).

In order to highlight the instability in the estimation algorithm only due to parameter mismatch, Fig. 15 shows system response of the PWM rectifier imposing that the parameter identification error is 20% and neglecting the presence of the PWM filter and of the line impedance. In this way, we can show the instability problem due to the parameter mismatch independently of the contribution given by the input filter dynamics. We can see that during the regenerative mode, the estimated voltage is clearly unstable and this instability occurs precisely at half of the switching frequency, as predicted in our analysis. The effect of the use of a pass-band filter in the estimation algorithm is shown in Fig. 16 where the oscillatory behaviour due to parameter mismatch has been removed. We also verified that, introducing the dynamics of the input filter and of the line impedance, but still considering the parameter mismatches, the system behaviour is very similar to that presented in Fig. 14, as long as, the current reference is generated using the adopted provisions.

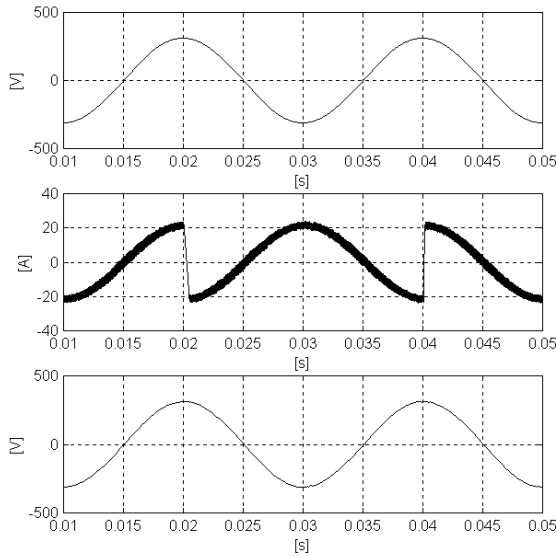


Fig. 16 PWM rectifier behaviour with the band-pass filter in the estimation algorithm and $\Delta L_{\%} = 20\%$. Upper trace: line voltage (u_s). Middle trace: converter output current ($-i_F$). Lower trace: estimated voltage (e_s).

6. CONCLUSIONS

The paper has presented a theoretical analysis of the stability robustness of the digital dead-beat current control technique with respect to parameter and model mismatches. These are very likely to be encountered when considering a PWM rectifier application of a current controlled, voltage-source converter. In particular, after presenting the results of the analysis concerning the parameter mismatch problem, the paper has focused on the interaction between the controlled rectifier and the input high frequency passive filters, which are not normally accounted for in the control's algorithm. Also for this case the proposed analysis technique effectively enables to predict the occurrence of instability problems, revealing the different robustness levels of the possible implementations of the converter's dead-beat control. The key role of the line voltage estimation technique in determining the control's robustness has been evidenced and a novel estimation strategy, which guarantees a superior performance level, has been proposed. This solution consists in decoupling the estimation algorithm both from the current reference

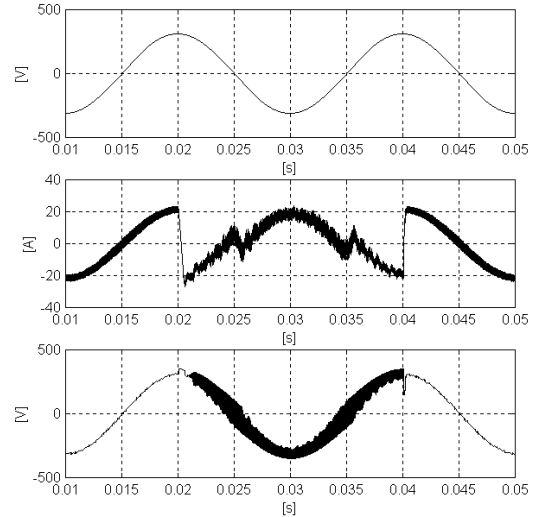


Fig. 15 PWM rectifier behaviour with the conventional estimation technique and $\Delta L_{\%} = 20\%$. Upper trace: line voltage (u_s). Middle trace: converter output current ($-i_F$). Lower trace: estimated voltage (e_s).

generation and from the dead-beat modulation algorithm. The effect is achieved by means of a simple band-pass digital filter on the estimated voltage. The effectiveness of the theoretical analysis and of the proposed improvements has been verified by simulations.

Acknowledgment

The authors thank Dr. A. Capuano for his help in verifying the theoretical analysis.

References

- [1] T. Kawabata, T. Miyashita, Y. Yamamoto: "Dead Beat Control of Three Phase PWM Inverter". IEEE Trans. on Power Electronics, vol. 5 No. 1, January 1990, pp. 21-28.
- [2] D.G. Holmes, D.A. Martin "Implementation of Direct Digital Predictive Current Controller for Single and Three Phase Voltage Source Inverters", IEEE IAS Conf. Rec., 1996, pp. 906-913.
- [3] T.G. Habetler: "A Space Vector-Based Rectifier Regulator for AC/DC/AC Converters". IEEE Trans. on Power Electronics, vol. 8 No. 1, January 1993, pp. 30-36.
- [4] K.P.Gokhale, A.Kawamura and R.G.Hoft: "Dead beat microprocessor control of PWM inverter for sinusoidal output waveform synthesis", IEEE

Trans. on Industry Application, vol. IA-23, No.5,
Sept./Oct. 1987, pp.901-909.

- [5] S. Buso, L. Malesani, P. Mattavelli: "Dead-Beat Current Control for Active Filters" IECON'98, Aachen, Germany, August 31-September 4, 1998, in press.
- [6] L. Malesani, P. Mattavelli, S. Buso: "Robust Dead-Beat Current Control for PWM Rectifiers and Active Filters", IEEE Industry Application Society (IAS) Annual Meeting, St. Louis, October 12-15, 1998, pp. 1377-1384.
- [7] A. Kawamura, T. Haneyoshi and R.G. Hoft: "Deadbeat controlled PWM inverter with parameter estimation using only voltage sensor". IEEE PESC'86 Conf. Rec., 1986, pp.576-583.
- [8] Y. Sato, T. Kataoka: "A Current-Type PWM Rectifier with Active Damping Function", IEEE Trans. on Industry Applications, Vol. 32 No. 3, May/June 1996 pp. 533-541.